Symbiont diversity and light-organ morphology in *Sepiola affinis*

Clotilde Bongrand, Raphael Lami, Marcelino T. Suzuki, and Eric J. Koch*

Sorbonne Université, CNRS, UMR8176 Laboratoire de Biodiversité et Biotechnologies Microbiennes (LBBM) 66650 Banyuls-sur-Mer, France

Running title: The *Sepiola affinis* light organ symbiosis.

*Communicating author: Eric J. Koch, ejkoch@hawaii.edu

The authors declare no competing financial interests.

Keywords: symbiosis, squid-vibrio symbiosis, mutualism, squid, *Vibrio spp*.

Abstract

The squid-vibrio symbiosis has illuminated fundamental mechanisms of beneficial animal-microbe associations, yet the interactions within sepiolid squid in the Mediterranean Sea remain underexplored. Here we characterize the *Sepiola affinis* squid-vibrio symbiosis by combining whole-genome sequencing of light-organ isolates, confocal microscopy, and temperature-dependent growth assays. Comparative genomic analyses (ANI, phylogenomics, and functional analyses) revealed two previously undescribed *Vibrio* species associated with the *S. affinis* light organ. One species clusters more distantly from other *Vibrio* while the other species is closer to established *Vibrio* clades, with the second species exhibiting an expanded repertoire of mobile elements and Type VI secretion components, suggesting heightened capacity for genetic exchange and interbacterial interaction. Confocal microscopy of juvenile squid established that the *S. affinis* light organ comprises twelve crypts connected by pores and ducts, expanding the number of symbiotic niches relative to other sepiolid squid. In addition, fluorescently labeled isolates from the two *Vibrio* species colonized juveniles in both mono- and co-colonization patterns within crypts. Finally, growth assays across 16–24°C identified species-specific temperature differences, indicating temperature preference that may align with seasonal variability in the Mediterranean Sea. Together, these findings position *S. affinis* as a tractable model for studying how symbiont diversity, organ architecture, and interbacterial interactions contribute to the stability of a mutualistic symbiosis.

Introduction

Animals and microbes routinely form symbiotic relationships that provide benefits for both partners [1]. These mutualisms are oftentimes integrated into aspects of host physiology such as development, immunity, and nutrition [2]. However, their inherent complexity presents a challenge for understanding the mechanisms underlying their stability. One way of addressing these challenges is through invertebrate models of symbiosis [3]. The partnership between sepiolid squid (i.e., bobtail squid) and bioluminescent *Vibrio (Aliivibrio)* bacteria (i.e., the squid-vibrio symbiosis) has served as a model for beneficial symbioses for more than 30 years [4–6]. Primarily known for research with the Hawaiian bobtail squid *Euprymna scolopes* and its symbiont *Vibrio fischeri*, the symbiosis has yielded groundbreaking insights into how animals and bacteria initially form and subsequently maintain a mutually beneficial relationship. In addition, sepiolid squid occur throughout the world's oceans, and many of them contain symbiotic associations with bioluminescent bacteria [7].

The most well-known symbiosis between sepiolid squid and *Vibrio* bacteria occurs within a dedicated light organ (Figure 1). When the squid first hatch, they are nonsymbiotic and acquire their bacterial symbiont from the surrounding environment [8]. The planktonic *Vibrio* migrate through sets of pores on both sides of the light organ, with each pore connecting to a duct and then ending at an epithelium-lined crypt [9]. The bacteria proliferate within the crypts, establishing symbiont populations that will remain for the lifespan of the squid. Within these crypt spaces, the host provides nutrients to the

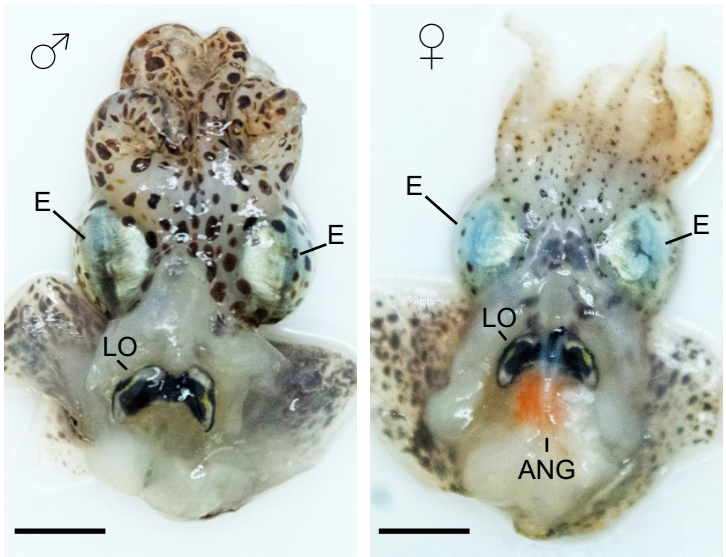

Figure 1. *Sepiola affinis* anatomy. Ventral dissections of a male (left) and a female (right); eyes (E) and light organ (LO) are indicated in both, and the accessory nidamental gland (ANG) is indicated in the female. Scale bars = 0.5 cm. Photographs courtesy of Alice Rodrigues.

bacteria in exchange for bioluminescence that is used as counterillumination during nocturnal activity [10]. In both *E. scolopes* and *Euprymna berryi*, the bilaterally symmetrical light organ contains a total of six crypts (i.e., three on each side), while the *Sepiola robusta* light organ has two additional crypts for a total of eight [11–13].

Numerous studies have examined the diversity of the bacteria colonizing the light organ [14, 15]. In *E. scolopes*, only *V. fischeri* has been found to naturally colonize, however, there is variation at the strain level of symbionts [16]. In addition to genomic analyses, behavioral diversity among *V. fischeri* strains during colonization has also been characterized [17–19]. Furthermore, similar behaviors during colonization of *E. scolopes* are exhibited in *V. fischeri* strains isolated from other hosts, including the Japanese squid *Euprymna morsei*, suggesting conserved colonization mechanisms [20]. The light organ in *E. Berryi* can also be colonized by *V. fischeri* [13]. Interestingly, sepiolid squid from the Mediterranean Sea harbor multiple species of *Vibrio* symbionts within their light organ [21]. Specifically, both *S. robusta* and *Sepiola affinis* are colonized by *V. fischeri* and other *Vibrio spp.* [21–23]. Because of the diversity exhibited in the light organ of Mediterranean sepiolid squid, we chose to examine the squid-vibrio symbiosis within *S. affinis*.

In this study, we characterized bacterial species and examined the morphology of the *S. affinis* light organ, yielding two main findings. First, whole genome sequencing was performed on light organ symbionts, allowing for the discovery of two uncharacterized species of *Vibrio* bacteria. In addition, *S. affinis* were successfully maintained in the laboratory, allowing for the production of hatchlings and subsequent colonization with labeled bacterial strains. This allowed characterization of the *S. affinis* juvenile light organ morphology, which led to the finding that the *S. affinis* light organ contains a total of twelve symbiotic crypt spaces. These findings show the greater diversity found within the *S. affinis* light organ relative to other squid light organs and further establish it as a promising model system to study the squid-vibrio symbiosis. Continuing to explore the *S. affinis* symbiosis can bring unique insights to the evolution and ecology of mutualistic associations.

Material and methods

Ethics Statement

All live animal collection, husbandry, and experiments were conducted in accordance with Sorbonne Universities and the Centre National de la Recherche Scientifique (CNRS) animal welfare protocols. All maintenance, rearing, and experimental procedures with the squid adhered to the animal welfare standards of EU Directive 2010/63 on the use of animals for scientific purposes. In France, the Observatoire Océanologique has an official ethical commission agreement (A6601601) to ensure that animal welfare standards are maintained.

S. affinis Husbandry

Adult *S. affinis* were collected at night during diving expeditions at ~20 m of water depth near Banyuls-sur-Mer, France. The squid were maintained at the Observatoire Océanologique in 30 l aquariums with flowing natural seawater that varied with the seasonal temperatures (e.g., ~13°C in winter to ~24°C in summer). The animals were maintained on a 12 h:12 h light:dark lighting schedule and fed live shrimp every night. Every morning, the aquariums were inspected and any eggs laid were removed, rinsed 3 x 10 min in filtered sterilized ocean water (FSOW) and then transferred to an aquarium with 5 l of FSOW and continuous aeration. The egg clutches were housed in individual aquariums and underwent a 50% water change every day and maintained at ~23°C. Upon hatching, the squid were removed and placed into fresh FSOW.

Bacterial isolation

All bacterial strains used in this study were isolated from field-caught *S. affinis* collected during trips in May, June, and July of 2022. To sample the light organ symbionts, each squid was briefly rinsed 3 x 5 min in 0.22 µm FSOW, anesthetized using 2% EtOH in FSOW, and then euthanized by increasing the concentration of EtOH to 4%. The central core tissues from the light organ, which contain the symbiotic crypts, were dissected out, combined for each squid in 70% FSOW, and homogenized using a pestle to release the bacteria. Half of the bacteria

133 were immediately mixed with glycerol diluted for a final concentration of 20% and frozen at
134 -80°C, while the remaining homogenate underwent serial dilutions that were then grown on
135 LBS agar [24] plates at three temperatures: 4°C, 20°C, and 25°C. Following incubation for 24
136 h (20°C and 25°C) or 5 d (4°C), ~100 total colonies were selected from each light organ across
137 the temperatures with a focus on selecting bacteria that displayed different size or color. Each
138 colony was transferred from the agar plate to liquid LBS using a toothpick and grown at 25°C
139 with 100 RPM shaking. After 24-48 h, cultures that exhibited visible growth had a subsample
140 removed, to which glycerol was added to a final concentration of 20%, and were frozen at -
141 80°C to create stocks.
142
143 *Whole genome sequencing*
144 Genomic DNA was extracted from cultures grown in LBS during exponential phase using the
145 DNeasy blood and tissue kit (QIAgen) according to the manufacturer's protocol. The quantity
146 and quality of gDNA extracted was measured using a Quantus fluorometer and a Denovix
147 DS11 Spectrophotometer, respectively. Twelve samples (four isolates per light organ from
148 each of three squid) were then sent to Plasmidsaurus (Eugene, OR) for whole genome
149 sequencing using Oxford Nanopore technology, assembly, and annotation. As part of the
150 analysis by Plasmidsaurus, all genomes underwent taxonomic analysis using Sourmash v4
151 and Mash [25, 26]. In addition, the Genome Taxonomy Database GTDP-tk was also used to
152 characterize the taxonomy of each genome [27, 28]. Average nucleotide identity (ANI) analysis
153 using FastANI v1.34 was performed against reference genomes of the top matches from
154 Sourmash, MASH, and GTDB-tk, in addition to various other *Vibrio* strains [29]. An ANI
155 similarity >95% was used to define the same species while >99.9% ANI similarity indicated the
156 same strain, which were combined for further analyses [29]. Digital DNA-DNA hybridization
157 (dDDH) was performed with the online Genome to Genone Distance Calculator [30, 31]. To
158 construct a phylogenetic tree of the distinct strains used in the ANI analysis, Orthofinder 3.0
159 was used with default parameters in combination with RAxML-NG [32, 33]. After establishing
160 the taxonomy, a Roary analysis with a 90% identity threshold was used to define genes that

161 were shared or distinct among the newly-isolated strains [34]. To compare gene functions,
162 eggNOG-mapper 2.1.12 was used for a COG analysis [35].
163
164 *Bacterial strains and labeling.*
165 The strains used in this study are listed in Table S1. Cultures were revived from -80°C stocks
166 and grown overnight in LBS medium. For confocal imaging, strains were fluorescently labeled
167 using triparental mating [36] with plasmids pVSV208 (red fluorescent protein) or pVSV102
168 (green fluorescent protein) [37]. Where appropriate, the medium was supplemented with
169 chloramphenicol (2.5 µg ml^{-1}) for pVSV208 or kanamycin (100 µg ml^{-1}) for pVSV102.
170
171 *Colonization procedure*
172 Bacterial strains were started from -80°C glycerol stocks onto two LBS agar plates and grown
173 overnight at either 20°C or 25°C. Individual colonies were transferred into 5 ml of LBS and
174 grown overnight 20°C or 25°C with 100 RPM shaking. The following morning, the culture with
175 the highest level of growth as determined by Optical Density at 600 nm (OD_{600}) was diluted
176 1:1000 into SWT (700 ml of FSOW, 300 ml H_20, 10 g NaCl, 5 g Bacto-Tryptone and 3 g yeast
177 extract) and incubated at 23°C with 100 RPM shaking and a standard colonization procedure
178 was followed [38]. When the bacteria had reached OD_{600} ~0.6, the culture was serially diluted
179 in FSOW 1:10,000 for a final concentration of ~10,000 bacteria ml^{-1} in 150 ml of FSOW. For
180 inoculations with two bacterial strains, each strain was first diluted to an OD_{600} ~0.6 and then
181 both added at concentrations of ~5,000 CFU ml^{-1}, for a total of ~10,000 bacteria ml^{-1}. Within
182 12 h of hatching, *S. affinis* were added to the inoculum and maintained overnight with a water
183 temperature of ~23°C. Following inoculation, the squid were rinsed 3 x 15 min in FSOW and
184 then maintained in FSOW.
185
186 *Confocal microscopy*
187 Squid were briefly anesthetized with 2% EtOH in seawater and then fixed with 4%
188 paraformaldehyde in mPBS (50 mM sodium phosphate buffer with 0.45 M NaCl, pH 7.4) for

189 12 h at 4°C. After fixation, the squid were rinsed 3 x 15 min in mPBS, the mantle opened and
190 light organ dissected out, and stained for 12 h with TOPRO-3 (Thermofisher Scientific) at a
191 dilution of 1:1000 in mPBS and rhodamine phalloidin (Thermofisher Scientific) at a dilution of
192 1:40 in mPBS. Samples were rinsed 3 x 20 min at room temperature with gentle rotation and
193 then mounted on glass slides in SlowFade Glass (Thermofisher Scientific). Imaging was
194 performed on a Leica Sp8 Confocal Microscope within the BioPIC platform at the Observatoire
195 Océanologique de Banyuls-sur-Mer. Post-imaging analysis and preparation for publication
196 was performed with FIJI [39], 3D-Slicer [40], and Imaris software (Oxford Instruments).
197
198 *Temperature Growth Assays*
199 Strains were initially grown on LBS agar, then serial dilutions were grown overnight in LBS,
200 and the dilution at OD_{600} ~1.0 for each strain was used further. For growth assays, the
201 equivalent of OD=0.05 for each strain was used to inoculate 1500 ul SWT and loaded in each
202 well of a 24-well plate. For each strain, three biological replicates (separate cultures grown on
203 different days) were assayed, each with three technical replicates. Plates were incubated with
204 continuous orbital shaking at 16°C, 20°C, or 24°C, and OD_{600} was recorded every 30 min for
205 10 h and again at 12 h and 24 h on a SpectraMax iD3 (Molecular Devices). To calculate growth
206 rates, OD values were natural-log transformed, and exponential-phase growth rates were
207 estimated by simple linear regression from 2–12 h. Growth rates were compared by two-way
208 ANOVA with a Tukey's multiple-comparisons correction in GraphPad Prism v10.6.0. An
209 adjusted P-value < 0.05 was considered significant.
210
211
212
213
214

Results

Symbiotic Vibrio spp. from S. affinis

To examine bacterial diversity within *S. affinis*, 100 strains were isolated from each light organ of three field-caught light organs (i.e., 300 total isolates). The genomic DNA was extracted from twelve total isolates (i.e., four isolates per light organ) and sent for whole genome sequencing. The sequencing results yielded a total of eleven high-quality genomes, with one sample being excluded because of quality issues. Initial ANI analysis to compare each strain revealed that four of the genomes were nearly-identical to another sample (ANI>99.9%), and in these cases only one strain was used in this study (Figure 2A). In total, seven distinct strains were obtained from three adults: two strains from each of two adults and three strains from the third adult (Table S1). The genomes of these strains span from 4.3 to 4.6 Mb and all exhibit a GC content of 39%. The seven genomes grouped into two clusters (consisting of three and four genomes), with 98–99% ANI similarity, indicating that strains within each grouping represent the same species. Using the definition that > 95% ANI similarity represents the same species [29, 41], further analysis against *Vibrio* reference genomes confirmed that the strains

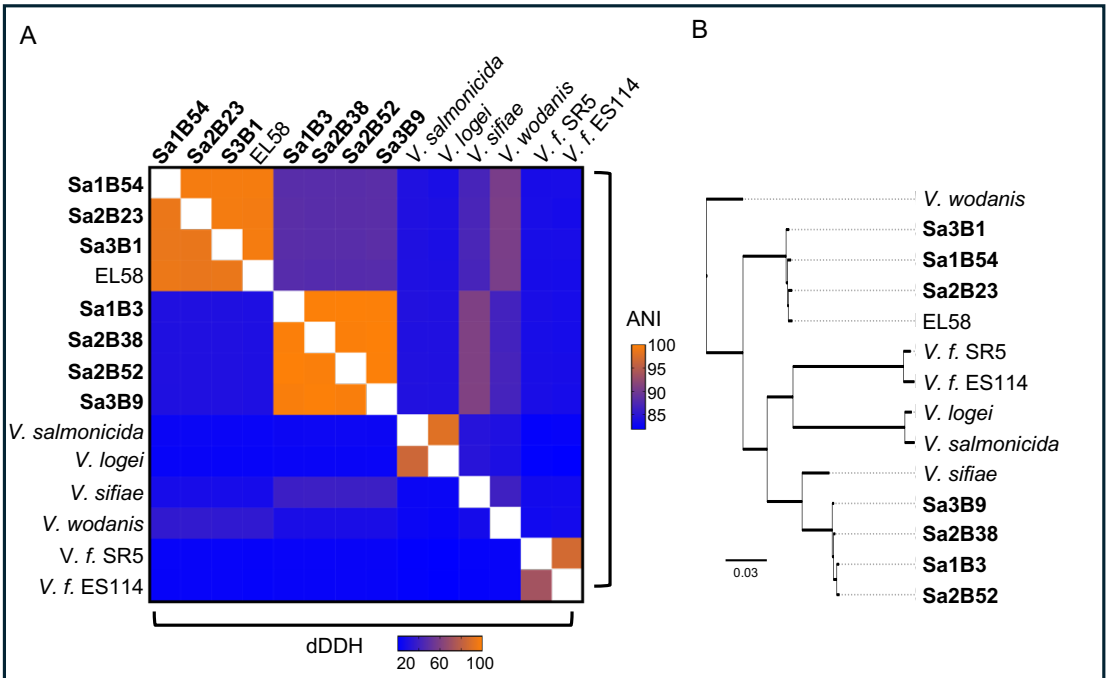

Figure 2. Relatedness of the *S. affinis* isolates. Strains isolated in this study are shown in bold. *V. f.* represents *Vibrio fischeri.* A) Heatmap of Average Nucleotide Identity (ANI; top) and digital DNA–DNA hybridization (dDDH; bottom) among *Vibrio* spp. strains, with colors ranging from higher similarity (orange) to lower similarity (blue). B) Maximum-likelihood phylogenetic tree inferred from 2,008 single-copy *Vibrio* genes using OrthoFinder and RAxML. The scale bar indicates the number of nucleotide substitutions per site.

230 are part of the genus *Vibrio* but, surprisingly revealed that none of the isolates were identified
231 as *V. fischeri* nor *V. logei* (Figure 2A). Furthermore, none of the (Alii)*Vibrio* reference genomes
232 exhibited ANI similarity > 95% with the *S. affinis* strains, and the most similar was *Vibrio*
233 *wodanis* at ~92% ANI similarity. However, the first grouping of 3 strains (hereafter referred to
234 as Banyuls_Sp1) exhibited ANI similarity of ~98% with a strain named EL58, indicating that
235 they are from the same species. The bacterial strain EL58 was isolated in 2015 from a
236 gorgonian coral in Faro, Portugal and identified as an *Aliivibrio sp.* [42]. The second grouping
237 of four strains (hereafter referred to as Banyuls_Sp2) exhibited no ANI similarity >95%, with
238 the highest similarity being with *Vibrio sifiae (92%)*. In addition to ANI analysis, dDDH
239 reinforced the finding that the strains belonged to two species that did not share species-level
240 similarity with other known *Vibrio* bacteria (dDDH > 70% indicate the same species) (Figure
241 2A, bottom). These results led to the conclusion that that the newly-isolated strains from the
242 *S. affinis* light organ belong to two separate novel *Vibrio* species.

243 To further investigate the similarity of the *S. affinis* strains relative to other *Vibrio*
244 species, Orthofinder in combination with RAxML-NG was used to construct a phylogenetic tree
245 from single-copy orthologs present in all of the genomes [32, 33] (Figure 2B). As expected
246 from the ANI analysis, Banyuls_Sp1 clustered closely with EL58 and the clade separated
247 themselves from the reference genomes, providing evidence of being from a distinct *Vibrio*
248 species. In contrast, Banyuls_Sp2 clustered more closely to the *Vibrio* reference strains, with
249 the closest being *Vibrio sifiae,* a bioluminescent bacterium originally isolated from surface
250 seawater in Tokyo Bay, Japan [43]. While all strains within Banyuls_Sp2 clustered tightly
251 together, their positioning among the reference genomes indicates that the species is more
252 similar genomically to the other *Vibrio spp*. than Banyuls_Sp1. Overall, these results show that
253 the bacterial strains isolated from the *S. affinis* light organ for this study represent two
254 previously undescribed species of *Vibrio* that share a symbiotic lifestyle.
255
256
257

258 *Comparative analyses of the Vibrio* spp.

259 To further characterize the two *Vibrio* species, a Roary analysis was performed to compare
260 gene presence and absence (Figure 3). Because of the ~90% ANI similarity between the two
261 species, we lowered the identity threshold for a shared gene from the default of 95% to 90%,
262 as has been demonstrated in other studies that examine across different species [44]. The
263 seven genomes contained 3913-4274 genes. From these genes, the Roary analysis built a
264 pangenome consisting of 8107 total genes (Figure 3A). Within the pangenome, all seven
265 strains shared 2088 genes (~26%), which constitute the core genome. Between the two *Vibrio*
266 species, there were 1228 (~15%) and 1344 (~17%) genes specific to Banyuls_Sp1 and
267 Banyuls_Sp2, respectively. Among the individual strains, there were on average 196 to 455
268 (~2%-6%) singletons or strain-specific genes.

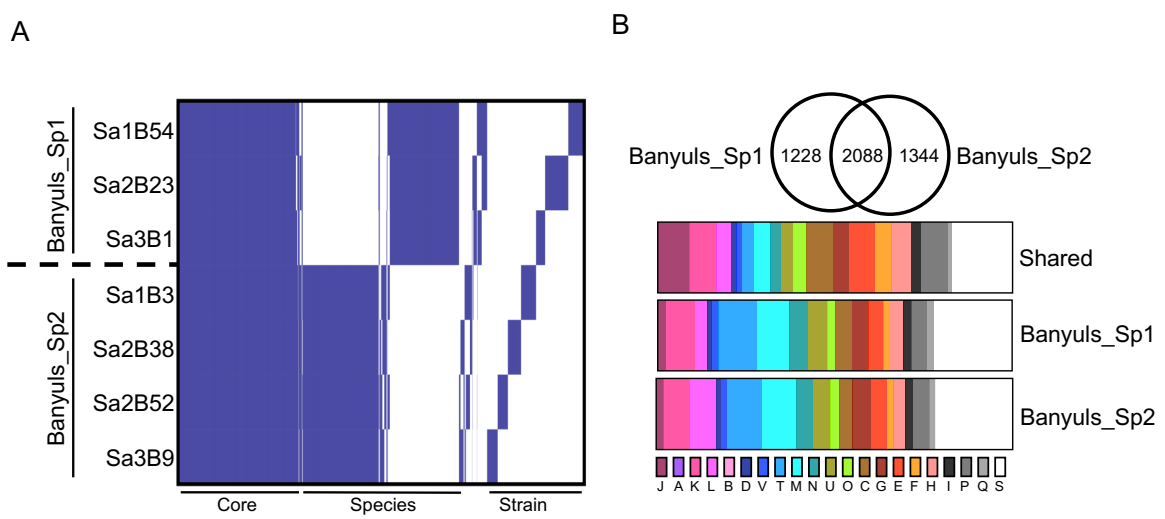

Figure 3. Comparison of two *Vibrio* spp. co-occurring in the *S. affinis* light organ. A) Roary presence/absence matrix for genes across the seven newly isolated symbiont strains. The two species have 2,088 shared genes (Core), ~1,300 species-specific genes (Species), and 161–411 strain-specific genes (Strain). B) Distribution of Clusters of Orthologous Groups (COG) assignments for genes from the Roary analysis. Top: comparison of COG distributions between the two *Vibrio* spp.; bottom: distribution by COG category. COG categories: J: Translation, ribosomal structure and biogenesis; A: RNA processing and modification; K: Transcription; L: Replication, recombination and repair; B: Chromatin structure and dynamics; D: Cell cycle control, cell division, chromosome partitioning; M: Cell wall/membrane/envelope biogenesis; V: Defense mechanisms; N: Cell motility; T: Signal transduction mechanisms; U: Intracellular trafficking, secretion, and vesicular transport; O: Posttranslational modification, protein turnover, chaperones; C: Energy production and conversion; G: Carbohydrate transport and metabolism; E: Amino acid transport and metabolism; F: Nucleotide transport and metabolism; H: Coenzyme transport and metabolism; I: Lipid transport and metabolism; P: Inorganic ion transport and metabolism; Q: Secondary metabolites biosynthesis, transport and catabolism; S: Function unknown.

269 After establishing patterns of gene presence and absence among the two *Vibrio*
270 species, a COG analysis by EggNOG was performed to compare functionality of the core and
271 species-specific genes (Figure 3B). Among the core genes, the COG categories J (Translation,

272 ribosomal structure and biogenesis), C (Energy production and conversion), E (amino acid
273 transport and metabolism), H (Coenzyme transport and metabolism) and P (Inorganic ion
274 transport and metabolism) are prevalent. This is expected as these categories represent basic
275 microbial processes that are highly conserved. Among the species-specific genes, the most
276 represented COG categories were T (Signal transduction mechanisms), M (Cell
277 wall/membrane/envelope biogenesis), N (Cell motility) and U (Intracellular trafficking,
278 secretion, and vesicular transport). In addition, Banyuls_Sp2 exhibited 180 genes belonging
279 to L (Replication, recombination and repair) compared to 129 genes in Banyuls_Sp1. Among
280 these L-category genes in Banyuls_Sp2, there were numerous genes related to transposase
281 activity and Group II introns. The prevalence of transposase and group II intron genes indicates
282 elevated mobile-element activity, consistent with high genetic transfer and a capacity to
283 diversify its genome [45]. In addition, while not consistently found in the same COG category,
284 Banyuls_Sp2 harbors a larger Type VI secretion system (T6SS) repertoire: 36 T6SS-
285 associated genes are present in all four Banyuls_Sp2 genomes, whereas only strain Sa2B23
286 from Banyuls_Sp1 encodes 13 T6SS genes and the other two strains have no annotated T6SS
287 components. These results suggest that Banyuls_Sp2 has higher potential for bacterial cell-
288 cell communication and in DNA acquisition/exchange relative to Banyuls_Sp1.
289
290 *Influence of temperature on Vibrio spp. growth*
291 With the knowledge that bacterial strains isolated from the light organs of *Sepiola spp*. exhibit
292 fluctuations in growth rate according to temperature, it was next tested whether the newly-
293 isolated *Vibrio spp*. exhibit similar patterns [21]. The growth rates for all seven strains were
294 tested at 16°C, 20°C, and 24°C to simulate cold, medium, and warm temperatures,
295 respectively (Figure 4). The growth rates for all strains during log-growth were compared using
296 a two-way ANOVA and it was found that while the strains were not significantly different from
297 one another (p-value = 0.1380), temperature was a significant factor (p-value = 0.0037). In
298 addition, the strains belonging to Banyuls_Sp1 exhibited their highest growth rate at 16°C and
299 lowest at 24°C, indicating that the strains grow faster at the colder temperatures (i.e., 16°C >

300 20°C > 24°C). Only Sa3B1 exhibited statistical significance between growth at 16°C and 24°C
301 (adj. p-value < 0.05). For Banyuls_Sp2, the strain growth rates were highest at 20°C, but there
302 was variability with the other temperatures, with Sa1B3 growing slowest at 16°C but the other
303 three strains slowest at 24°C. None of these differences in growth rate were statistically
304 significant when comparing temperatures (adj. p-value > 0.05). These results indicate that the
305 newly-isolated *Vibrio spp*. exhibit subtle, yet consistent temperature-dependent differences in
306 growth rate.

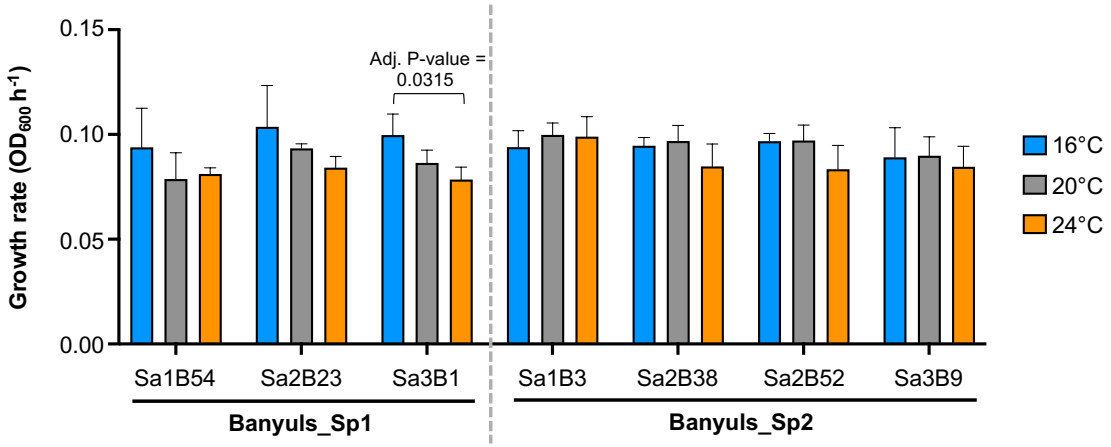

Figure 4. Effect of temperature on growth of *Vibrio* sp. strains. Growth rate for each strain measured at 16°C (blue), 20°C (grey), and 24°C (orange). Statistical significance of temperature effects within strains was tested by two-way ANOVA with multiple comparisons; brackets above indicate statistical significance between two growth rates. Error bars denote SD (n = 3).

307

308 *Morphology of the juvenile S. affinis light organ*

309 The exterior appearance of the juvenile *S. affinis* light organ is consistent with other sepiolid
310 squid [11, 12]. The *S. affinis* light organ is bilobed with a heart-shaped appearance and
311 contains two appendages on each side: a longer anterior appendage and a shorter poster
312 appendage (Figure 5A). At the base of each anterior appendage, a set of six pores occur that
313 lead inside the light organ (Figure 5C). The presence of twelve pores per light organ is more
314 than those present in *E. scolopes* and *E. berryi*, which have six pores, or *S. robusta*, which has
315 eight [9, 12, 13]. Each pore leads to a separate duct that terminates by connecting into a crypt
316 for a total of twelve distinct crypt spaces that will house the bacterial symbiont(s). To visualize
317 the interior of the juvenile squid colonized by symbionts, *S. affinis* were exposed to

318 fluorescently labelled
319 ES114, a well-studied *V.*
320 *fischeri* strain that has
321 stability harboring
322 fluorescent plasmids [46,
323 47]. Within the *S. affinis* light
324 organ, the crypts are
325 arranged in an overlapping
326 formation that makes
327 distinguishing them
328 challenging (Figure 5B,
329 Movie S1). The largest crypt
330 (Crypt 1) is the most medial
331 and closest to the ventral
332 surface (Figure 5D). Crypts
333 2-5 then progressively get
334 slightly smaller, more
335 lateral, and more dorsal
336 (Figure 5E-F). Crypt 6 is the
337 smallest, most lateral (i.e.,
338 closest to the pores and
339 appendages), and most
340 dorsal, but was often
341 partially or not colonized.

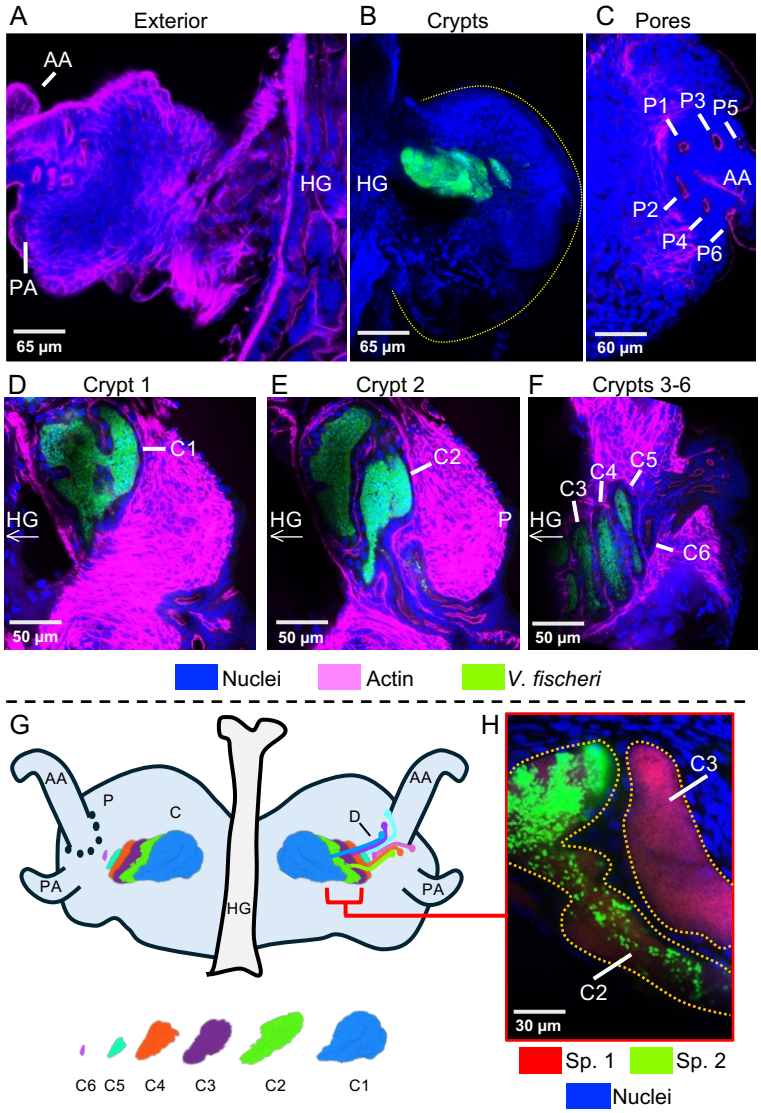

Figure 5. Juvenile light organ of *S. affinis* at 48 h post-colonization. Top row: (*A*) exterior view showing anterior (AA) and posterior appendages (PA) and hindgut (HG); (*B*) interior view with symbiont-containing crypts (green) and the light-organ outline (yellow dashed line); (*C*) pores (P1–P6). Middle row: (*D*) crypt 1 (C1), (*E*) crypt 2 (C2), (*F*) and crypts 3–6 (C3–C6); arrow indicates hindgut direction. Bottom row: (*G*) schematic of pores and crypts (leftside), with ducts (rightside), and individual crypts (below); (*H*) example of co-colonized (C2) and mono-colonized (C3) crypts containing newly isolated *Vibrio spp.* with Banyuls_Sp1 (Sp. 1) and Banyuls_Sp2 (Sp. 2). Scale bars, as indicated.

342 The six overlapping crypts create an overall architecture of near continuous symbiotic bacteria
343 that is slightly angled outwards due to the progression from ventral to dorsal (Figure 5G). After
344 initial characterization of the *S. affinis* light organ with ES114, some of the strains isolated from
345 *S. affinis* were labeled with a fluorescent plasmid and tested for colonization (Figure 5F).

346 Through confocal microscopy, it was established that Banyuls_Sp1 and Banyuls_Sp2 strains
347 colonize juvenile *S. affinis* when inoculated in pairs originating from the same host.
348 Furthermore, the *Vibrio spp*. were observed both in monocolonization and co-colonization of
349 crypt spaces. These results confirm that the newly-isolated Banyuls_Sp1 and Banyuls_Sp2
350 strains can colonize the *S. affinis* light organ and exhibit colonization patterns (e.g., both mono
351 and co-colonized crypts) similar to how *V. fischeri* strains colonize *E. scolopes* [19].
352
353 **Discussion**
354 Natural symbioses examined under laboratory conditions deepen the understanding of
355 how mutualistic associations operate within an ecological context [48, 49]. The squid-vibrio
356 symbiosis is a versatile model for natural animal-microbe mutualisms because it combines a
357 host that can be maintained under both symbiotic and nonsymbiotic conditions with a bacterial
358 partner that is highly tractable in the laboratory [50]. In addition, study of field-caught *E.*
359 *scolopes* and *V. fischeri* in their native habitat of Hawaii has allowed for incorporation of
360 ecological factors to provide a well-rounded perspective of environmentally-transmitted
361 symbioses [15, 17]. The Mediterranean Sea harbors a wide diversity of sepiolid squid globally,
362 providing a unique reservoir of squid-vibrio symbioses [7, 51]. Furthermore, with multiple
363 bacterial symbionts, the squid-vibrio symbiosis in *S. affinis* provides a unique perspective into
364 how bacterial species co-colonize and persist within the light organ. To better understand how
365 the squid-vibrio symbiosis functions with multiple bacterial species, this study aimed to assess
366 the microbial diversity and light organ morphology encountered within the sepiolid squid *S.*
367 *affinis*.
368 From the *S. affinis* light organ, two species of symbiotic *Vibrio* bacteria were isolated
369 and their genomes characterized. The discovery of these species highlights the value of whole
370 genome approaches in bacteria, especially in *Vibrio spp*. The finding of multiple *Vibrio* species
371 from *S. affinis* light organs was expected, as this was found in 1998 using 16S rRNA gene
372 sequences and two species were identified as *V. fischeri* and *Vibrio logei* [21]. Subsequently,
373 a study using a Multilocus Sequence Analysis (MLSA) approach confirmed the species identity

374 of some *Sepiola* light-organ isolates and reclassified others [23]. Other studies have used
375 different combinations of genes and genomes to examine the *Vibrio* taxonomy, highlighting
376 the complexity of the genus [28, 52]. One study in particular included the genome of EL58
377 isolated from a Mediterranean Sea coral and grouped it with *Sepiola spp*. light organ strains,
378 indicating that these strains represent a *Vibrio* species that exhibits a conserved role as a
379 bacterial symbiont [52].

380 In addition, it is worth noting the pattern of both species being present in all three light
381 organs examined for this study. The presence of multiple *Vibrio* species within *S. affinis and*
382 *S. robusta* light organs has been linked to temperature-dependent growth patterns that were
383 exhibited by each *Vibrio* species [21]. In contrast, *E. scolopes* is only colonized in its native
384 habitat of Hawaii by *V. fischeri.* Therefore, the presence of two *Vibrio* species with different
385 temperature preferences within *S. affinis* and *S. robusta* may be an adaptation to the larger
386 seasonal temperature fluctuations in the northwestern Mediterranean Sea relative to the
387 tropical waters surrounding Hawaii. However, the mechanisms of how the host is consistently
388 colonized by multiple species remains unknown. Further study of the newly characterized light
389 organ symbionts can advance our understanding of partner choice in different environments
390 with temperature variations, providing an intriguing contrast to tropical symbioses with more
391 constant conditions. Moreover, the *S. affinis* squid-vibrio symbiosis provides a tractable system
392 to investigate how climate change, specifically effects related to temperature increases, could
393 reshape marine host–microbe interactions.

394 The genomes of the seven *Vibrio* strains each exhibit ~4000 genes, which is typical
395 among *Vibrios*. Consistent within the *Vibrio* genus, strain-level diversity appears to be driven
396 by horizontal gene transfer and gene presence/absence variation [53–55], a phenomenon also
397 observed in other bacterial species present in horizontally acquired microbiomes [56, 57]. The
398 functional analysis of the genomes showed that Banyuls_Sp2 contained many genes related
399 to the exchange of genetic material (e.g., transposases and Group II intron family genes). The
400 finding of Group II intron genes is interesting because, to the best of our knowledge, this is the
401 first finding of the gene family in a light organ symbiont, whereas they are known to be present

402 in pathogenic *Vibrios* such as *Vibrio cholerae* and *Vibrio paraheamolyticus* [58]. In addition,
403 the higher prevalence of T6SS genes across all four Banyuls_Sp2 strains, relative to
404 Banyuls_Sp1, suggests an enhanced capacity for interbacterial interaction in the former.
405 Finally, the phylogenetic analysis provides further support for differences in genomic
406 composition between the two species (Fig. 2B). In the phylogenetic tree, Banyuls_Sp2 clusters
407 more closely with other *Vibrio spp*., indicating higher similarity, whereas Banyuls_Sp1 is
408 comparatively isolated. The higher similarity of Banyuls_Sp2 to the other *Vibrio spp*. may
409 reflect increased horizontal gene transfer (e.g., through transposases and Group II intron
410 family genes), while Banyuls_Sp1 appears more conserved. While this study provides a first
411 characterization of these symbiotic species, additional strains, symbiotic or planktonic, need
412 to be collected and sequenced to better capture the diversity of the species. Furthermore,
413 monitoring of the two species within the light organ across host maturation and seasons would
414 yield key insights into their colonization dynamics and stability.

415 Finally, to visualize the symbiosis within the *S. affinis* light organ, the two *Vibrio* species
416 were labeled with plasmids expressing a Green or Red fluorescent protein (i.e., GFP or RFP).
417 Strains of both species were able to be successfully transformed with the plasmids, which is a
418 reflection of the compatibility and plasticity of these *Vibrio* species. When visualizing the
419 juvenile light organs of *S. affinis*, the general structure is similar to *E. scolopes*, *E. berryi*, and
420 *S. robusta* with a bilobed organ that has ciliated appendages and a migration pathway
421 consisting of pores leading to ducts that terminate at crypts [9, 12, 13]. However, the *S. affinis*
422 light organ has twelve crypts, pores, and ducts, more than the six-eight present in the other
423 squid-vibrio symbioses that have been described. The presence of nearly twice as many crypts
424 provides more symbiotic niches for distinct populations of symbionts to grow. In *E. scolopes*,
425 crypts are colonized by a single strain most of the time and the presence of twice as many
426 crypts would provide opportunity for increased symbiont diversity. Thus, the greater number of
427 crypts within the *S. affinis* light organ could be an adaptation to increase symbiont diversity
428 and provide greater stability through seasonal fluctuations in the Mediterranean Sea. Upon
429 examination of the newly-characterized *Vibrio* strains within the *S. affinis* light organ, both

430 monocolonized crypts and co-colonized crypts were observed. These patterns of light organ
431 colonization are similar to those in *E. scolopes*, where *V. fischeri* strains can co-colonize the
432 same the same crypt or occupy different crypts [17, 18]. However, the number of light organs
433 examined was too low for quantitative analysis. Another difference within the *S. affinis* light
434 organ was the lack of clear antechambers in the ducts and bottlenecks at the entrance to the
435 crypts (Movie S1), which are distinct features of both *E. scolopes* and *E. berryi*. In *E. scolopes*,
436 the bottleneck has been linked to the daily venting behavior that occurs at dawn [59]. However,
437 the lack of a large diel venting cycle in the *S. affinis* light organ may be the reason for the
438 absence of the bottleneck, without a need to suddenly release the majority of the bacterial
439 population. In the bioluminescent Japanse Pinecone Fish *Moncentris japonica*, a similar
440 pattern of slow, continuous release of the bacterial symbionts with random larger pulses led
441 the authors to conclude that the bacterial populations grow continuously [60]. Future studies
442 of the native bacterial symbionts in *S. affinis* will provide evidence if there are species-
443 dependent patterns within the light organ crypts. It is important to sample more squid and
444 sequence more bacterial isolates to shed light on this symbiosis and be able to draw further
445 conclusions on the microbial diversity present in *S. affinis*.

446 In conclusion, we deliver an in-depth characterization of the *Sepiola affinis* squid-vibrio
447 symbiosis by examining the light-organ architecture and performing whole-genome analyses
448 of its bacterial symbionts. Whole-genome sequencing revealed two previously undescribed
449 *Vibrio* species within this symbiosis. Moreover, genome analyses indicate that one lineage is
450 comparatively distinct relative to other *Vibrio spp*., whereas the other species clusters with
451 prominent *Vibrio* clades and exhibits an expanded repertoire for genetic exchange and T6SS,
452 implying heightened interbacterial interaction. In parallel, we characterized the juvenile *S.*
453 *affinis* light-organ morphology, finding conserved migration pathways (pores→ducts→crypts)
454 similar to other squid light organs, yet an expanded number of crypts with twelve. Taken
455 together, these results support the hypothesis that the *S. affinis* squid-vibrio symbiosis
456 prioritizes symbiont diversity via twelve symbiotic niches and the presence of multiple
457 symbiotic *Vibrio* species

Acknowledgements

This work benefited from access to the Observatoire Océanologique de Banyuls-sur-Mer, an EMBRC-France and EMBRC-ERIC. The authors are grateful to the BOSS (https://www.obs-banyuls.fr/fr/observer.html) diving and boating services (for help with animal collection) and Aquariology services (helping maintain live animals) . We thank the Bio2Mar (https://bio2mar.obs-banyuls.fr) and BioPIC (https://www.obs-banyuls.fr/fr/rechercher/plateformes/biopic.html) core facilities for providing access to instrumentation and technical support. We thank Michael Fuentes of BIOM for help with maintaining live animals, and Dr. Stephanie Bertrand and Dr. Hector Escriva of BIOM for access to IMARIS software. Support was provided by Marie Skłodowska-Curie Actions under grant agreements No 101064524 to Dr. Eric Koch and No 101153902 to Dr. Clotilde Bongrand.

Conflict of Interest

The authors declare no conflicts of interest.

References

1. McFall-Ngai M, Hadfield MG, Bosch TC, et al. Animals in a bacterial world, a new imperative for the life sciences. *Proc Natl Acad Sci U S A* 2013;110:3229–3236.
2. Xu J, Gordon JI. Honor thy symbionts. *Proc Natl Acad Sci U S A* 2003;100:10452–10459.
3. Koch EJ, McFall-Ngai M. Model systems for the study of how symbiotic associations between animals and extracellular bacterial partners are established and maintained. *Drug Discov Today Dis Models* 2018;28:3–12.
4. Nyholm S V., McFall-Ngai MJ. A lasting symbiosis: how the Hawaiian bobtail squid finds and keeps its bioluminescent bacterial partner. *Nature Reviews Microbiology 2021 19:10* 2021;19:666–679.
5. Visick KL, Stabb E V., Ruby EG. A lasting symbiosis: how *Vibrio fischeri* finds a squid partner and persists within its natural host. *Nat Rev Microbiol* 2021;19:654–665.
6. Septer AN, Visick KL. Lighting the way: how the *Vibrio fischeri* model microbe reveals the complexity of Earth's "simplest" life forms. *J Bacteriol* 2024;206(5):e0003524.
7. Sanchez G, Fernández-Álvarez FÁ, Taite M, et al. Phylogenomics illuminates the evolution of bobtail and bottletail squid (order Sepiolida). *Commun Biol* 2021;4:819.
8. Nawroth JC, Guo H, Koch E, et al. Motile cilia create fluid-mechanical microhabitats for the active recruitment of the host microbiome. *Proc Natl Acad Sci U S A* 2017;114(36):9510–9516.
9. Sycuro LK, Ruby EG, McFall-Ngai M. Confocal microscopy of the light organ crypts in juvenile *Euprymna scolopes* reveals their morphological complexity and dynamic function in symbiosis. *J Morphol* 2006;267:555–568.

10. Ruby EG, McFall-Ngai MJ. A squid that glows in the night: development of an animal-bacterial mutualism. *J Bacteriol* 1992;174:4865.
11. Montgomery MK, McFall-Ngai M. Embryonic Development of the Light Organ of the Sepiolid Squid *Euprymna scolopes Berry*. *Biol Bull* 1993;184:296–308.
12. Foster JS, Von Boletzky S, Mcfall-Ngai MJ. A comparison of the development of *Sepiola robusta Naef* and *Euprymna scolopes Berry* (cephalopoda: Sepiolidae). *Bull Mar Sci* 2002;70:141–153.
13. Imes AM, Pavelsky MN, Badal K, et al. *Euprymna berryi* as a comparative model host for *Vibrio fischeri* light organ symbiosis. *Appl Environ Microbiol* 2025;91(8):e0000125.
14. Wollenberg MS, Ruby EG. Population structure of *Vibrio fischeri* within the light organs of *Euprymna scolopes* squid from Two Oahu (Hawaii) populations. *Appl Environ Microbiol* 2009;75:193–202.
15. Bongrand C, Koch E, Mende D, et al. Evidence of genomic diversification in a natural symbiotic population within its host. *Front Microbiol* 2022;13:854355.
16. Bongrand C, Ruby EG. The impact of *Vibrio fischeri* strain variation on host colonization. *Curr Opin Microbiol* 2019;50:15–19.
17. Wollenberg MS, Ruby EG. Phylogeny and fitness of *Vibrio fischeri* from the light organs of *Euprymna scolopes* in two Oahu, Hawaii populations. *ISME Journal* 2012;6:352–362.
18. Bongrand C, Koch EJ, Moriano-Gutierrez S, et al. A genomic comparison of 13 symbiotic *Vibrio fischeri* isolates from the perspective of their host source and colonization behavior. *ISME J* 2016;10:2907–2917.
19. Bongrand C, Ruby EG. Achieving a multi-strain symbiosis: strain behavior and infection dynamics. *ISME J* 2019;13:698–706.
20. Bongrand C, Moriano-Gutierrez S, Arevalo P, et al. Using colonization assays and comparative genomics to discover symbiosis behaviors and factors in *Vibrio fischeri*. *mBio* 2020;11:03407–19.
21. Fidopiastis PM, Von Boletzky S, Ruby EG. A new niche for *Vibrio logei*, the predominant light organ symbiont of squids in the genus *Sepiola*. *J Bacteriol* 1998;180:59–64.
22. Dunlap PV, Ast JC, Kimura S, et al. Phylogenetic analysis of host-symbiont specificity and codivergence in bioluminescent symbioses. *Cladistics* 2007;23(5):507–532.
23. Ast JC, Urbanczyk H, Dunlap P V. Multi-gene analysis reveals previously unrecognized phylogenetic diversity in *Aliivibrio*. *Syst Appl Microbiol* 2009;32:379–86.
24. Graf J, Dunlap P V., Ruby EG. Effect of transposon-induced motility mutations on colonization of the host light organ by *Vibrio fischeri*. *J Bacteriol* 1994;176:6986–6991.
25. Irber L, Tessa Pierce-Ward N, Abuelanin M, et al. sourmash v4: A multitool to quickly search, compare, and analyze genomic and metagenomic data sets. *J Open Source Softw* 2024;9:6830.
26. Ondov BD, Treangen TJ, Melsted P, et al. Mash Screen: High-throughput sequence containment estimation for genome discovery. *Genome Biol* 2019;20:1–13.
27. Chaumeil PA, Mussig AJ, Hugenholtz P, et al. GTDB-Tk v2: memory friendly classification with the genome taxonomy database. *Bioinformatics* 2022;38:5315–5316.
28. Parks DH, Chuvochina M, Rinke C, et al. GTDB: an ongoing census of bacterial and archaeal diversity through a phylogenetically consistent, rank normalized and complete genome-based taxonomy. *Nucleic Acids Res* 2022;50:D785–D794.
29. Jain C Rodriguez-R LM, Phillippy AM, et al. High throughput ANI analysis of 90K prokaryotic genomes reveals clear species boundaries. *Nat Commun* 2018;9:1–8.
30. Meier-Kolthoff JP, Auch AF, Klenk HP, et al. Genome sequence-based species delimitation with confidence intervals and improved distance functions. *BMC Bioinformatics* 2013;14:60.
31. Meier-Kolthoff JP, Carbasse JS, Peinado-Olarte RL, et al. TYGS and LPSN: a database tandem for fast and reliable genome-based classification and nomenclature of prokaryotes. *Nucleic Acids Res* 2022;50:D801–D807.

32. Emms DM, Kelly S. OrthoFinder: Phylogenetic orthology inference for comparative genomics. *Genome Biol* 2019;20:1–14.
33. Kozlov AM, Darriba D, Flouri T, et al. RAxML-NG: a fast, scalable and user-friendly tool for maximum likelihood phylogenetic inference. *Bioinformatics* 2019;35:4453–4455.
34. Page AJ, Cummins CA, Hunt M, et al. Roary: rapid large-scale prokaryote pan genome analysis. *Bioinformatics* 2015;31:3691–3693.
35. Cantalapiedra CP, Hernández-Plaza A, Letunic I, et al. eggNOG-mapper v2: Functional Annotation, Orthology Assignments, and Domain Prediction at the Metagenomic Scale. *Mol Biol Evol* 2021;38:5825–5829.
36. Stabb E V., Ruby EG. RP4-based plasmids for conjugation between *Escherichia coli* and members of the *vibrionaceae*. *Methods Enzymol* 2002;358:413–426.
37. Dunn AK, Millikan DS, Adin DM, et al. New *rfp*- and pES213-derived tools for analyzing symbiotic *Vibrio fischeri* reveal patterns of infection and *lux* expression in situ. *Appl Environ Microbiol* 2006;72:802–810.
38. Koch EJ, Bongrand C, Bennett BD, et al. The cytokine MIF controls daily rhythms of symbiont nutrition in an animal-bacterial association. *Proc Natl Acad Sci U S A* 2020;117:27578–27586.
39. Schindelin J, Arganda-Carreras I, Frise E, et al. Fiji: An open-source platform for biological-image analysis. *Nat Methods* . 2012. 2012. , 9: 676–682
40. Fedorov A, Beichel R, Kalpathy-Cramer J, et al. 3D Slicer as an Image Computing Platform for the Quantitative Imaging Network. *Magn Reson Imaging* 2012;30:1323–1341.
41. Konstantinidis KT, Tiedje JM. Genomic insights that advance the species definition for prokaryotes. *Proc Natl Acad Sci U S A* 2005;102:2567–2572.
42. Raimundo I, Silva SG, Costa R, et al. Bioactive secondary metabolites from octocoral-associated microbes-new chances for blue growth. *Mar Drugs* 2018;16:485.
43. Yoshizawa S, Karatani H, Wada M, et al. *Aliivibrio sifiae* sp. nov., luminous marine bacteria isolated from seawater. *J Gen Appl Microbiol* 2010;56:509–518.
44. Estrada AA, Gottschalk M, Gebhart CJ, et al. Comparative analysis of *Streptococcus suis* genomes identifies novel candidate virulence-associated genes in North American isolates. *Vet Res* 2022;53:23.
45. Zhao C, Pyle AM. Crystal structures of a group II intron maturase reveal a missing link in spliceosome evolution. *Nature Structural & Molecular Biology 2016 23:6* 2016;23:558–565.
46. Koch EJ, Miyashiro T, McFall-Ngai MJ, et al. Features governing symbiont persistence in the squid-vibrio association. *Mol Ecol* 2014;23:1624–1634.
47. Koch EJ, Moriano-Gutierrez S, Ruby EG, et al. The impact of persistent colonization by *Vibrio fischeri* on the metabolome of the host squid *Euprymna scolopes*. *J Exp Biol* 2020;223:jeb212860.
48. Ruby EG. Symbiotic conversations are revealed under genetic interrogation. *Nat Rev Microbiol* 2008;6:752–762.
49. Bosch TCG, Guillemin K, McFall-Ngai M. Evolutionary “Experiments” in symbiosis: The study of model animals provides insights into the mechanisms underlying the diversity of Host–Microbe interactions. *BioEssays* 2019;41:1800256.
50. Nyholm SV, McFall-Ngai M. The winnowing: establishing the squid–vibrio symbiosis. *Nat Rev Microbiol* 2004;2:632–642.
51. Bello G. The Mediterranean Sepiolidae (Mollusca Cephalopoda) diversity. *Biodivers J* 2019;10:389–404.
52. Klemetsen T, Karlsen CR, Willassen NP. Phylogenetic Revision of the Genus Aliivibrio: Intra- and Inter-Species Variance Among Clusters Suggest a Wider Diversity of Species. *Front Microbiol* 2021;12:626759.
53. Chibani CM, Roth O, Liesegang H, et al. Genomic variation among closely related *Vibrio alginolyticus* strains is located on mobile genetic elements. *BMC Genomics* 2020; 21(1):354..

606 54. Levade I, Terrat Y, Leducq JB, et al. *Vibrio cholerae* genomic diversity within and
607 between patients. *Microb Genom* 2017;3:*e000142*.
608 55. Lin H, Yu M, Wang X, et al. Comparative genomic analysis reveals the evolution and
609 environmental adaptation strategies of *vibrios*. *BMC Genomics* 2018;19:135.
610 56. Vatanen T, Plichta DR, Somani J, et al. Genomic variation and strain-specific
611 functional adaptation in the human gut microbiome during early life. *Nat Microbiol*
612 2018;4:470–479.
613 57. Picazo DR, Werner A, Dagan T, et al. Pangenome evolution in environmentally
614 transmitted symbionts of deep-sea mussels is governed by vertical inheritance.
615 *Genome Biol Evol* 2022.
616 58. Candales MA, Duong A, Hood KS, et al. Database for bacterial group II introns.
617 *Nucleic Acids Res* 2012;40.
618 59. Essock-Burns T, Bongrand C, Goldman WE, et al. Interactions of symbiotic partners
619 drive the development of a complex biogeography in the Squid-Vibrio symbiosis. *mBio*
620 2020;11(3):e00853-20.
621 60. Haygood MG, Tebo BM, Nealson KH. Luminous bacteria of a monocentrid fish
622 (*Monocentris japonicus*) and two anomalopid fishes (*Photoblepharon palpebratus* and
623 *Kryptophanaron alfredi*): population sizes and growth within the light organs, and rates
624 of release into the seawater. *Mar Biol* 1984;78:249–254.
625

626 **Supplemental Figure Legends**

627

628 **Movie S1**. Juvenile light organ of *S. affinis* at 48 h post-colonization with *V. fischeri* ES114

629 (green). The positioning of the hindgut (HG) and pores are indicated for orientation as well as

630 the visible crypts (C1-C6), ducts (D1-D6), and pores (P1-P4). Counterstains are for actin

631 (magenta) and nuclei (nuclei). Scale bar, as indicated.

632

633 **Table S1**. Strains used in the study.

634

635